

Article

Comparison of Individual Tree Height Estimated from LiDAR and Digital Aerial Photogrammetry in Young Forests

Arun Gyawali ^{1,*}, Mika Aalto ¹, Jussi Peuhkurinen ², Maria Villikka ² and Tapio Ranta ¹

¹ Laboratory of Bioenergy, Lappeenranta-Lahti University of Technology LUT, Lönnrotinkatu 7, 50100 Mikkeli, Finland; mika.aalto@lut.fi (M.A.); tapio.ranta@lut.fi (T.R.)

² Arbonaut Oy, Kaislaku 2, 80130 Joensuu, Finland; jussi.peuhkurinen@arbonaut.com (J.P.); maria.villikka@arbonaut.com (M.V.)

* Correspondence: arun.gyawali@lut.fi

Abstract: Biomass stored in young forests has enormous potential for the reduction of fossil fuel consumption. However, to ensure long-term sustainability, the measurement accuracy of tree height is crucial for forest biomass and carbon stock monitoring, particularly in young forests. Precise height measurement using traditional field measurements is challenging and time consuming. Remote sensing (RS) methods can, however, replace traditional field-based forest inventory. In our study, we compare individual tree height estimation from Light Detection and Ranging (LiDAR) and Digital Aerial Photogrammetry (DAP) with field measurements. It should be noted, however, that there was a one-year temporal difference between the field measurement and LiDAR/DAP scanning. A total of 130 trees (32 Scots Pine, 29 Norway Spruce, 67 Silver Birch, and 2 Eurasian Aspen) were selected for height measurement in a young private forest in south-east Finland. Statistical correlation based on paired t-tests and analysis of variance (ANOVA, one way) was used to compare the tree height measured with the different methods. Comparative results between the remote sensing methods and field measurements showed that LiDAR measurements had a stronger correlation with the field measurements and higher accuracy for pine ($R^2 = 0.86$, bias = 0.70, RMSE = 1.44) and birch ($R^2 = 0.81$, bias = 0.86, RMSE = 1.56) than DAP, which had correlation values of ($R^2 = 0.71$, bias = 0.82, RMSE = 2.13) for pine and ($R^2 = 0.69$, bias = 1.19, RMSE = 2.08) for birch. The correlation of the two remote sensing methods with the field measurements was very similar for spruce: LiDAR ($R^2 = 0.83$, bias = 0.30, RMSE = 1.17) and DAP ($R^2 = 0.83$, bias = 0.44, RMSE = 1.26). Moreover, the correlation was highly significant, with minimum error and mean difference ($R^2 = 0.79$ – 0.98 , MD = 0.12–0.33, RMSD = 0.45–1.67) between LiDAR and DAP for all species. However, the paired t-test suggested that there is a significant difference ($p < 0.05$) in height observation between the field measurements and remote sensing for pine and birch. The test showed that LiDAR and DAP output are not significantly different for pine and spruce. Presumably, the time difference in field campaign between the methods was the reason for these significant results. Additionally, the ANOVA test indicated that the overall means of estimated height from LiDAR and DAP were not significantly different from field measurements in all species. We concluded that utilization of LiDAR and DAP for estimating individual tree height in young forests is possible with acceptable error and comparable accuracy to field measurement. Hence, forest inventory in young forests can be carried out using LiDAR or DAP for height estimation at the individual tree level as an alternative to traditional field measurement approaches.

Keywords: young forest; LiDAR; digital aerial photogrammetry; Individual tree detection; canopy height model; tree height



Citation: Gyawali, A.; Aalto, M.; Peuhkurinen, J.; Villikka, M.; Ranta, T. Comparison of Individual Tree Height Estimated from LiDAR and Digital Aerial Photogrammetry in Young Forests. *Sustainability* **2022**, *14*, 3720. <https://doi.org/10.3390/su14073720>

Academic Editor: Marc A. Rosen

Received: 24 December 2021

Accepted: 19 March 2022

Published: 22 March 2022

Publisher's Note: MDPI stays neutral with regard to jurisdictional claims in published maps and institutional affiliations.



Copyright: © 2022 by the authors. Licensee MDPI, Basel, Switzerland. This article is an open access article distributed under the terms and conditions of the Creative Commons Attribution (CC BY) license (<https://creativecommons.org/licenses/by/4.0/>).

1. Introduction

In 2020, the share of renewable energy sources in Finnish end consumption was 40%, of which wood fuels alone contributed 29% to the nation's energy demand, and they are,

thus, the most used single energy source in Finland [1]. The 50% target for renewable energy in Finland's National Energy and Climate Strategy for 2030 is likely to further increase demand for forest biomass for energy production, and it is estimated that demand for wood chips for energy use could double by 2030, which would necessitate harvesting of energy wood throughout the country [2]. Against this background, the government of Finland is promoting more active young forest management and encouraging forest owners to undertake small tree harvesting. In addition, the Ministry of Agriculture and Forestry has presented proposals for the provision of incentives for seedling planting, young forest management and silvicultural operations through the METKA (Metsätalouden kannustejärjestelmä) incentive scheme for forestry [3] as the production of energy woods is not economically feasible without these kinds of support programs [4]. Statistics show that Finland has a considerable amount of biomass stored in young forests (i.e., forests at the stage where they are in need of first thinning) and greater utilization of this source can supply substantial amounts of wood fuel and bioenergy, which will help Finland meet its renewable energy targets [5].

In Finland, forest resource information data is collected by the Finnish forest center (Suomen metsäkeskus) based on combined light detection and ranging (LiDAR), aerial photography, and field measurements of circular sample plots. The forest inventory output is in the form of 16×16 m raster grid squares covering the whole country [6]. The forest resource information collected by the Finnish forest center is open data. Moreover, Finnish forest owners receive inventory information about forest plot characteristics such as volume, growing stock, time of first thinning, etc., at the stand level. On a regional scale, remote sensing is the main source of data collection for forest inventory in Nordic countries [7]. At the forest plot scale, however, inventory information at the individual tree level is essential for planning forest management activities, and information on tree height is very important when forest owners and managers are making decisions on silvicultural activities.

Precision in height measurement of trees is crucial for assessing above-ground biomass (AGB) in young forests, but tree height measurement is relatively difficult regardless of the method used, be it field measurement or a remote sensing method [8]. It should be noted that field measurement of tree height is more difficult than diameter measurement because of the nature of branches and tree crowns, and optical effects [9]. Furthermore, traditional approaches to field measurement of tree parameters are very time consuming and labor intensive, and the accuracy of field-measured height remains uncertain until measured from the felled trees [10]. Biometric factors such as tree species, age, length of the fallen tree, topography, and stand structure also influence the accuracy of field measurements of tree height [11].

Remote sensing (RS) methods such as terrestrial laser scanning (TLS), mobile laser scanning (MLS), airborne laser scanning (ALS), unmanned aerial vehicle (UAV) LiDAR, and digital aerial photogrammetry (DAP) have proved to be efficient and accurate for estimating tree parameters [12–19]. In recent years, UAV LiDAR has become increasingly popular [20–26] as it provides 3D information with a higher spatial resolution due to its low flying altitude [27–29]. It also accommodates a higher data acquisition frequency for continuous forest monitoring and offers high temporal resolution [30]. Moreover, it has been found that LiDAR processing algorithms are robust and standardized, and elevation data is accurate [31]. The detection rate of individual trees and the crown height estimation are also very accurate [32–34]. However, the cost of scanning and data acquisition are the major limitations for LiDAR application in forest inventory [35].

Interest in DAP in forest inventory has similarly grown significantly because of its ability to provide 3D point clouds and acceptable accuracy [36–38] and the lower cost of data acquisition and processing [39,40] compared to LiDAR. UAV-DAP can provide accurate information about individual tree height [19,41–43] by using differences in structure from motion (SfM) software data in image processing [44,45]. In addition, high-density SfM point clouds have been found helpful for monitoring canopy structures of boreal forests with

long temporal and large spatial extent [46]. Research has also shown that forest inventory can be successfully carried out using photogrammetrically derived drone-based image point clouds (DIPC) even without in-situ field measurement [47]. Hence, the application of high-resolution DAP can be considered a reliable alternative to LiDAR for collecting information on the forest structure [48,49].

Earlier studies have commonly used either LiDAR or DAP data to study forest resources, but only a small number of studies [23,32,33,38,45,50–53] have compared the performance of both methods simultaneously for the estimation of forest structural parameters. It should be noted, however, that these previous studies have mainly focused on mixed, uneven-aged, and mature forests. Nevertheless, a few studies in which the height of an individual tree is accurately estimated in small plantation trees utilizing LiDAR [54–57] and DAP [19,41,42,58–60] have been presented. In addition to these, some very limited studies have been carried out comparing UAV LiDAR and DAP tree height on small horticultural tree crops [61], young plantation forest [62], and Eucalyptus trees of varying age and tree height ranging from 5 m to 16 m [45].

Chao et al. [63] reviewed five estimation methods using remote sensing information for energy crop biomass evaluation. They aggregated remote sensing data from LiDAR and DAP to acquire physical proxies of plant biomass such as crop height in agriculture. However, to the best of our knowledge, no work can be found in the literature that compares individual tree height estimations between UAV LiDAR and digital aerial photogrammetry in fully grown young energy wood forests. This study aims to address this research gap by utilizing both UAV LiDAR and DAP data to estimate and compare individual tree height in a low-density young Finnish forest. The work aims to answer the research question of whether DAP and LiDAR can be utilized as a tree height measurement method for young forest inventory.

2. Materials and Methods

2.1. Study Area

The study area is located in a private forest in Pieksämäki ($62^{\circ}21'0''$ N $27^{\circ}6'30''$ E) in the Southern Savonia region of Finland, Figure 1.

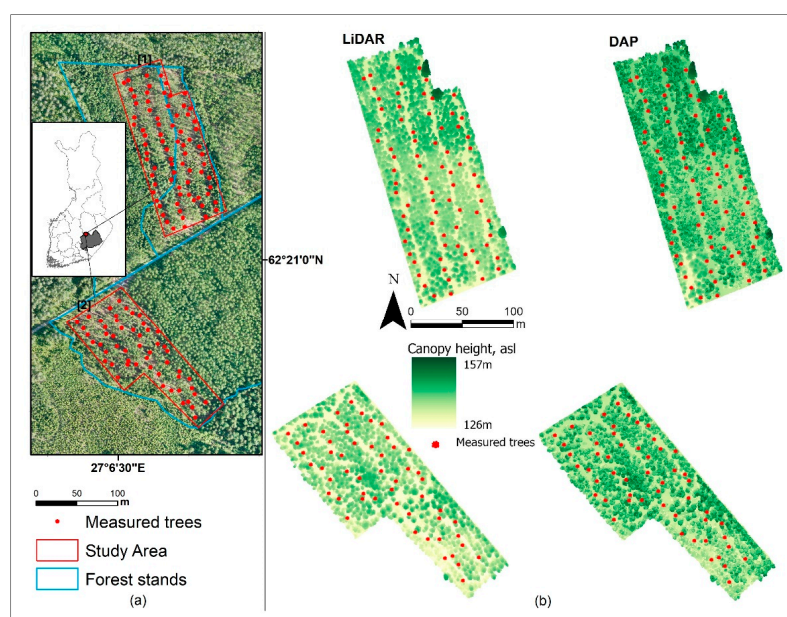


Figure 1. Study area: (a) Finland showing the Southern Savonia region and study area with location of field-measured trees, and (b) LiDAR and DAP point clouds.

The selected study area (2.8 ha) is located within three forest stands. We took the forest stands boundaries from the open access forest data published by the Finnish Forest Centre.

We defined the forest stand as young forest because of its age, the mean diameter at breast height (DBH), and the mean height of the trees [64], and because the plot had recently undergone its first commercial thinning operation for forest bioenergy [65]. The three forest stands were regrouped into two study stand areas based on the stand characteristics. The study area in the northern two stands was designated as stand area 1 and that of the southern stand as stand area 2 (Figure 1). The stand attributes of the forest studied are presented in Table 1. The shape of the study area was delineated based on the trail left by the harvesting machine.

Table 1. Attributes of forest stands located in the study area as defined by the Finnish Forest Centre [64].

Stands	Area (ha)	Stand Age (year)	Developmental Class	Dominant Species	Mean DBH (cm)	Mean Height (m)
1	3.12	25	Young forest	Scots Pine	10.30	9.50
2	6.18	27	Young forest	Silver Birch	13.68	13.16

2.2. DAP Data

The digital aerial photographs used in the study were taken on 16 June 2020. The DAP images were acquired using a 42 MP Sony RX1R II (Sony, Tokyo, Japan) compact camera with a GEODRONE X4L drone (Geotrim Oy, Vantaa, Finland). This drone can resist a maximum of 18 m/s of wind speed and the flight range can reach up to 2500 m. A single flight was conducted for capturing photographs. The flight path of the UAVs for both LiDAR and DAP was controlled by a predefined ground control system. The GNSS and inertial measurement unit (IMU) in the drone recorded the longitude and latitude, elevation, roll angle, and pitch angle of each image in real-time. The five ground control points (GCPs) were set within the study area and were located using Trimble RTK (Real-Time Kinematic) positioning. The spatial resolution of the photographs was 4 cm/pixel. Image overlaps were 80 % for longitudinal and 65 % for lateral sections. A total of 812 images were captured during flight in the area. Here, the area means a larger area captured from the UAV, of which the study area is a part. All images had a photo resolution of 7952 × 5304 pixels.

2.3. LiDAR Data

The UAV LiDAR campaign took place on 29 July 2020, one and half months after the DAP scanning, using the same UAV as used for DAP image collection. The LiDAR data were acquired by a YellowScan Surveyor[®] sensor (YellowScan SAS, Saint-Clément-de-Rivière, France). The system comprises a Velodyne VLP-16 Puck laser scanner, a high-performance Global Navigation Satellite System (GNSS) antenna, and an Inertial Navigation System (INS). These features enable highly accurate position and orientation determination and direct georeferencing. The point cloud data from LiDAR was classified into ground and non-ground points. The flying parameters for both LiDAR and DAP are presented in Table 2. More information related to LiDAR and DAP is provided in Figure 1 and Appendix A, Figures A1–A3.

Table 2. LiDAR and DAP flying parameters.

Parameters	LiDAR	DAP
Flying height (m)	60	140
Average Flying speed (m/s)	5	7
Point density (points/m ²)	105	NA *
Pulse rate (kHz)	300	NA *
Overlap in flight direction (%)	NA *	80
Side overlap (%)	50	65
Distance between flight lines (m)	50	27

* Not Applicable.

2.4. Validation Field Data Collection

Reference data were collected on the 10 and 14 June 2021, one year after the LiDAR–DAP campaign, and are given in the appendix (Figure A4). A total of 130 individual trees from the three stands were sampled for height measurement. The area had previously undergone harvesting operations by machine harvester (Ponsse Scorpion King). Eight straight corridors were marked after the harvesting, and we used these corridors as a straight line for our measurement. Systematic sampling was conducted, and the nearest tree (right or left) was measured at 10-m intervals along the line. High-precision GNSS was not required to locate individual tree positions. Instead, we utilized the LiDAR and DAP tree list map (polygon and point map) and high-resolution orthophotographs to locate the individual trees in the field. Moreover, the tree density of the study area was sparse (LiDAR-1020 trees/ha and DAP-996 trees/ha according to our RS scanning result for all three stands) because of the harvesting operation. Field height measurement was carried out only of those trees that had been detected in both the LiDAR and DAP scanning and were present in the tree list map. The tree height was measured using a Suunto PM5/1520 clinometer (Suunto Oy, Finland). The dominant tree species in all three forest stands were Scots Pine (*Pinus sylvestris*), Norway Spruce (*Picea abies*), and Silver Birch (*Betula pendula*). Planted Eurasian Aspen (*Populus tremula*) also coexisted as a secondary species in all stands. There is a discrepancy in time between the field measurement and drone campaign. The time difference is one growing season with a height growing period of May–July. In addition, previous study has indicated that trees mostly grow in height rather than diameter during their young age [66]. Hence, we expected to find a slightly higher height from field measurement than found with the LiDAR and DAP measurements.

2.5. DAP and LiDAR Processing for CHM

For DAP analysis, the transformation of images into digital maps and 3D point clouds was performed using the professional software Pix4D (Pix4D S.A. Prilly, Switzerland) [67]. The structure from motion algorithm in Pix4D was used in aerial imagery pre-processing to generate dense image point clouds. The average point density of the area was 732 pts/m². Both data sets, LiDAR and DAP point clouds, were normalized by the LiDAR-generated digital elevation model (DEM) to derive heights above ground. A canopy height model (CHM) was created based on the normalized point cloud using the method presented by Khosravipour et al. [68] for both DAP and LiDAR. The method has two stages. In the first stage, standard a CHM is created using all first returns and partial CHMs from the first returns that correspond to higher-up vegetation hits. Note that in DAP data all returns are first returns. In the second stage, the CHMs are combined into one CHM based on the highest value across all CHMs for each x and y raster position. The pixel size of CHM for both LiDAR and DAP was 20 cm × 20 cm. The CHMs from LiDAR and DAP are shown in Figure 2.

2.6. Estimation of Height from DAP and LiDAR

Individual tree crowns were delineated from the DAP and LiDAR-derived CHM (Figure 3) separately using the automatic tree delineation method built-in ArboLiDAR (Arbonaut Oy Ltd., Joensuu, Finland) [69]. The first step is to preprocess the CHM by filling the small holes in the CHM and masking out small vegetation, in our case vegetation below 2.0 m. Local maxima were then searched from the CHM and a region growing method was applied to these seed points. The polygons delineated with the method were converted to points that represented tree locations. The height of an individual tree was estimated to be the highest observation from the point cloud inside the polygon.

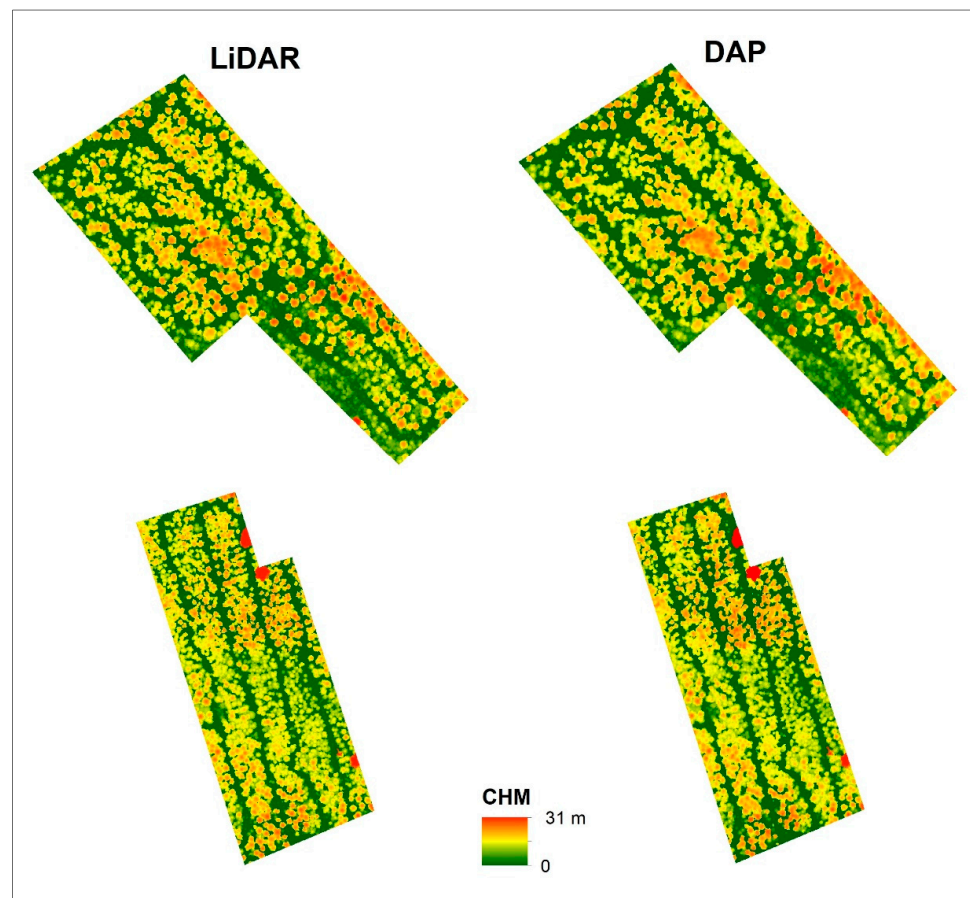


Figure 2. Canopy height model constructed from LiDAR and DAP in the study area.

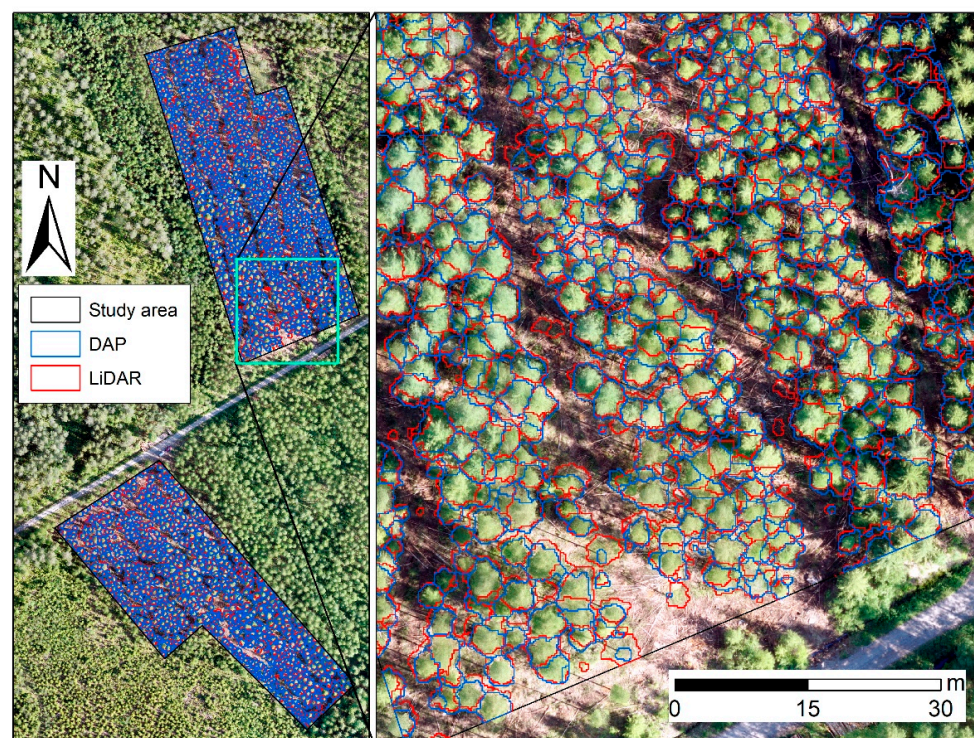


Figure 3. LiDAR and DAP tree crown delineation from CHM.

2.7. Data Analysis

First, correlation of the height of an individual tree from all three combinations, i.e., field measurement vs. DAP, field measurement vs. LiDAR, and LiDAR vs. DAP was carried out. The coefficient of determination (R^2) was calculated to find the correlation between all pairs using Equation (1). Further, we calculated root mean square error (RMSE) and bias for height accuracy assessment of field-LiDAR and field-DAP using Equations (2) and (3). For LiDAR-DAP, the root mean square deviation (RMSD) and mean difference (MD) were computed in a similar manner to the RMSE and bias, respectively.

$$R^2 = 1 - \frac{\sum_{i=1}^n (x_i - \hat{x}_i)^2}{\sum_{i=1}^n (x_i - \bar{x}_i)^2} \quad (1)$$

$$\text{RMSE} = \sqrt{\frac{1}{n} \sum_{i=1}^n (x_i - \hat{x})^2} \quad (2)$$

$$\text{bias} = \frac{1}{n} \sum_{i=1}^n (x_i - \hat{x}_i) \quad (3)$$

where x_i represents the field-measured values for tree i , \hat{x}_i represents the estimated values for tree i , \bar{x}_i represents the average field-measured values for all trees, and n is the total number of trees.

Next, the height differences were calculated from three measurements to check the range of the differences. The mean difference, standard deviation, and minimum and maximum values of the differences were calculated for all species to ascertain whether tree heights derived from one method were, on average, greater or smaller than those of other methods. The normality of the height differences (residuals) was tested using the Shapiro-Wilk test. Further, comparative analyses of the three methods were carried out using both paired t-tests and one-way analysis of variance (ANOVA).

3. Results

3.1. Descriptive Results

Information on the height observed with the three methods is presented in boxplots in Figure 4. Aspen is omitted from the figure since there were only two observations of aspen trees during the field campaign. Due to the time difference between the remote sensing and field campaigns, the mean height from field measurement is, as expected, higher for all species.

Details of the descriptive statistics are shown in Table 3. The field measurements resulted in heights ranging from 7 to 26 m with a mean value of 13 m for all species, whereas LiDAR and DAP gave heights ranging from 5 to 26 m with a mean of 12 m. Among the 130 individual trees, pine was found to have the shortest and tallest tree based on the field measurements. On the other hand, LiDAR and DAP found birch and pine to have the shortest and tallest tree, respectively. The standard deviation for pine is greater than that of the other species with standard deviation ranging from 3.1–3.3 m observed for all methods. The minimum standard deviation value is found for aspen (0.5–1 m) because there are only two close height readings (16 and 18 m) for this species.

Table 3. Descriptive results of height (m) derived from field measurements, LiDAR, and DAP.

Species	Field Measurement			LiDAR			DAP		
	Mean (SD)	Min	Max	Mean (SD)	Min	Max	Mean (SD)	Min	Max
Pine ($n = 32$)	11.23 (3.25)	6.50	25.50	10.53 (3.52)	5.30	25.80	10.42 (3.64)	5.10	25.70
Spruce ($n = 29$)	12.26 (2.66)	7.50	19.00	11.98 (2.82)	6.00	19.40	11.83 (2.89)	5.20	19.60
Birch ($n = 67$)	13.68 (2.84)	7.50	19.50	12.82 (2.94)	5.20	20.10	12.49 (3.06)	5.00	19.00
Aspen ($n = 2$)	17.00 (0.71)	16.50	17.50	16.70 (1.27)	15.80	17.60	16.45 (0.50)	16.10	16.80
All ($N = 130$)	12.82 (3.10)	6.50	25.50	12.13 (3.22)	5.20	25.80	11.89 (3.30)	5.00	25.70

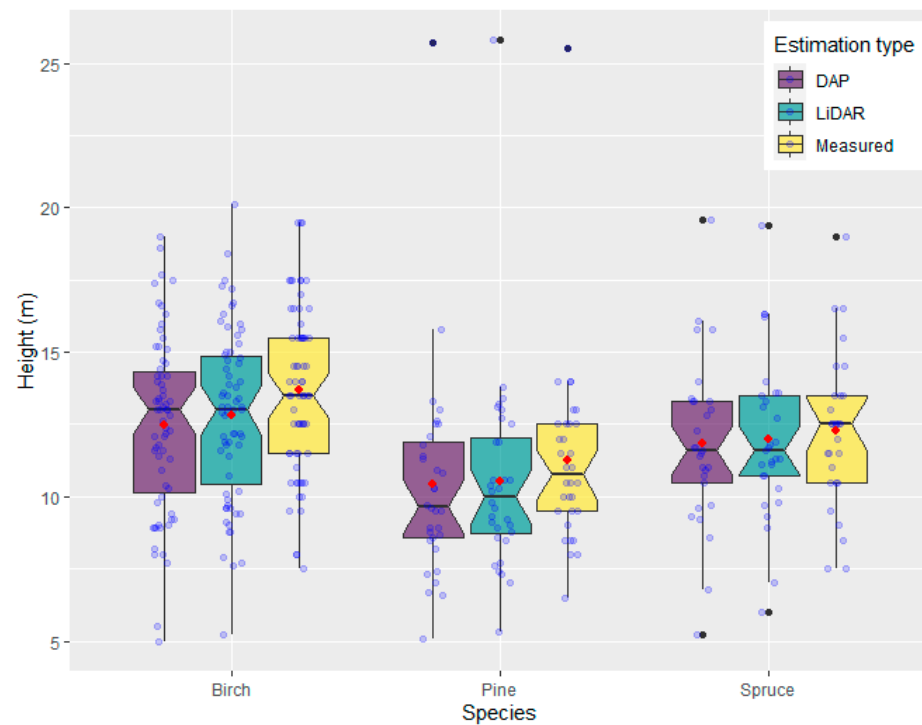


Figure 4. Box plot showing tree height information with mean height (red points) derived from the three methods used. The total number of trees (N) is 128 (Pine = 32, Spruce = 29 and Birch = 67 and Aspen(omitted) = 2).

3.2. Correlation Analysis

Correlation analysis was performed for individual tree height measured and estimated from each combination of field measurement, LiDAR and DAP for pine, spruce, and birch, which resulted in nine outputs. Scatter plots in Figure 5 show the nine correlation outputs.

The comparison of the field, LiDAR, and DAP tree height for the three species is summarized in Table 4. The obtained R^2 values, error (RMSE or RMSD), and bias or MD showed a good correlation between the field, LiDAR, and DAP tree height observations. The R^2 values are 0.85 (Measured vs. LiDAR), 0.70 (Measured vs. DAP), and 0.86 (LiDAR vs. DAP) for all species. LiDAR values are more closely correlated with measured height than DAP values in all species. The error associated with LiDAR is smaller than the error obtained for DAP in all three species. Interestingly, spruce has lower error (Bias= 0.30 and RMSE= 1.17) and higher correlation ($R^2 = 0.83$) with measurement data, which are very comparable and minimum errors shown by LiDAR. In addition, the LiDAR–DAP relationship is strongest among the three pairs, followed by Measured–LiDAR when combining all species. Similarly, for all species, the LiDAR–DAP pair has the lowest MD and RMSD values, whereas Measured–DAP shows the highest RMSE and bias.

Table 4. Correlation and errors of tree height derived from the field, LiDAR, and DAP data for different species.

Species	Measured vs. LiDAR			Measured vs. DAP			LiDAR vs. DAP		
	R^2	Bias	RMSE	R^2	Bias	RMSE	R^2	MD	RMSD
Pine	0.86	0.70	1.44	0.71	0.82	2.13	0.79	0.12	1.67
Spruce	0.83	0.30	1.17	0.83	0.44	1.26	0.98	0.15	0.45
Birch	0.81	0.86	1.56	0.69	1.19	2.08	0.85	0.33	1.26
All	0.85	0.67	1.44	0.70	0.92	1.92	0.86	0.24	1.25

Note: Pearson's correlation among the three pairs was statistically significant for all species at $p < 0.01$.

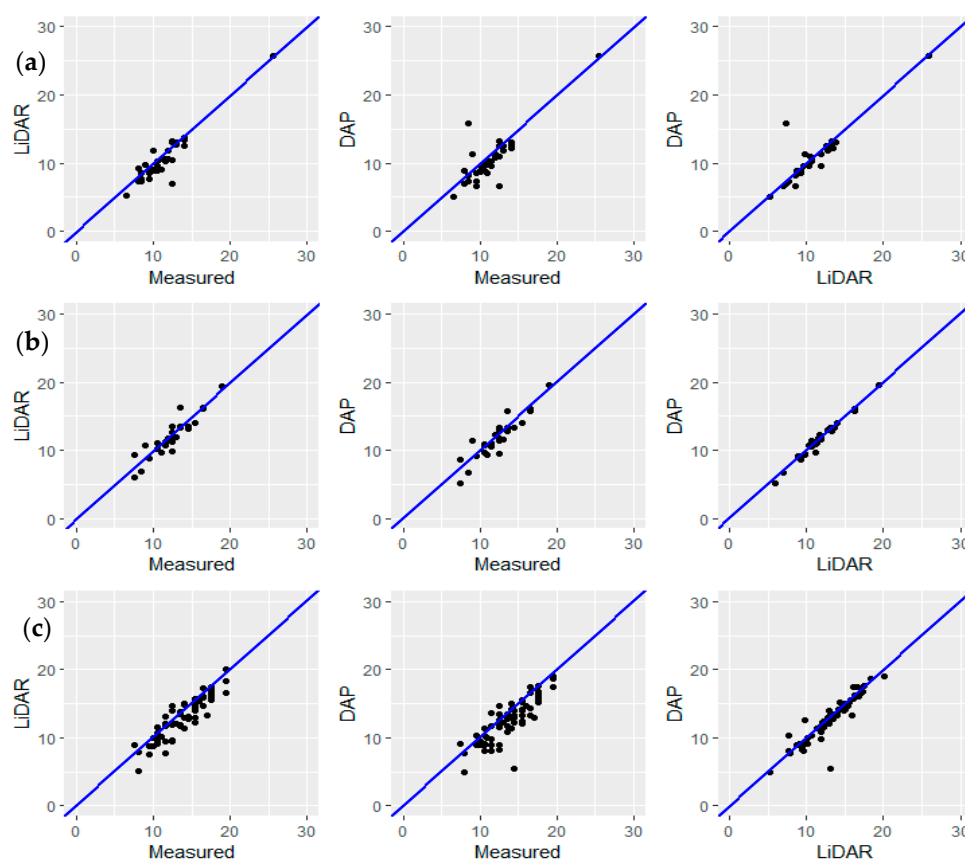


Figure 5. Scatter plots of height estimation (m) from LiDAR against field measurements, DAP against field measurements, and DAP against LiDAR for (a) pine, (b) spruce, and (c) birch.

3.3. Height Differences

3.3.1. Descriptive Results

Height differences between field vs. remote sensing methods are presented in Table 5. In Measured vs. LiDAR height, the average height difference was 0.69 m. The minimum and maximum difference observed was in aspen (0.10 m) and pine (5.50 m), respectively. Similarly, in Measured vs. DAP height, the average height difference was 0.92 m, where the minimum difference was 0.40 m for aspen and the maximum difference was 9 m for birch. In LiDAR vs. DAP height, the minimum and maximum height differences were 0.30 m in aspen and 8.40 m in pine, respectively, with an average of 0.24 m. The maximum height difference of 5.50 m, 5.90 m, 7.30 m, 7.60 m, and 8.40 m was measured and calculated only from 3 (2 pine and 1 birch) out of 130 trees. The mean and SD values explained those maximum height differences well.

Table 5. Height differences (m) between field and remote sensing data.

Species	Measured–LiDAR			Measured–DAP			LiDAR–DAP		
	Mean (SD)	Min	Max	Mean (SD)	Min	Max	Mean (SD)	Min	Max
Pine	0.70 (1.28)	−1.90	5.50	0.82 (2.00)	−7.30	5.90	0.12 (1.69)	−8.40	2.40
Spruce	0.30 (1.15)	−2.80	2.70	0.44 (1.20)	−2.40	2.90	0.15 (0.43)	−0.70	1.40
Birch	0.86 (1.31)	−2.10	3.80	1.19 (1.71)	−2.20	9.00	0.33 (1.23)	−2.90	7.60
Aspen	0.30 (0.57)	−0.10	0.70	0.55 (0.21)	0.40	0.70	0.25 (0.78)	−0.30	0.80
All	0.69 (1.27)	−2.80	5.50	0.92 (1.69)	−7.30	9.00	0.24 (1.23)	−8.40	7.60

3.3.2. Normality of Residuals

A normality test of the height differences among the methods was performed using the Shapiro-Wilk test for all species. The test resulted [Pine- (Field measured-LiDAR: $W = 0.89$, $p = 0.003$; Field measured-DAP: $W = 0.77$, $p = 9.8 \times 10^{-6}$ and LiDAR- DAP: $W = 0.51$, $p = 3.2 \times 10^{-9}$), [Spruce- (Field measured-LiDAR: $W = 0.95$, $p = 0.24$; Field measured-DAP: $W = 0.96$, $p = 0.42$ and LiDAR- DAP: $W = 0.95$, $p = 0.19$)] and [Birch- (Field measured-LiDAR: $W = 0.99$, $p = 0.82$; Field measured-DAP: $W = 0.92$, $p = 0.0003$ and LiDAR- DAP: $W = 0.70$, $p = 1.7 \times 10^{-10}$)]. The $p > 0.05$ for all methods for spruce measurement and measured vs. LiDAR height for birch shows an indication of assumption of normal random error in residuals. The rest of the residuals were skewed from normal, as can be seen in the histogram of individual residuals and the normal curve for all species in Figure 6.

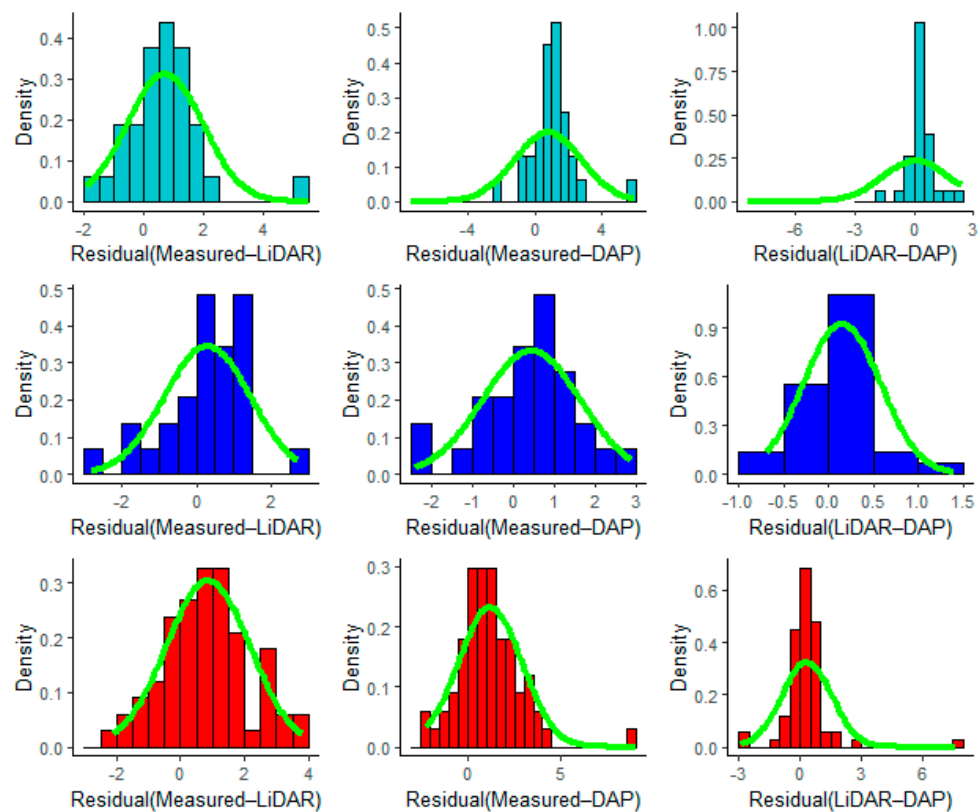


Figure 6. Histograms of height differences between methods in pine (turquoise), spruce (blue), and birch (red).

3.3.3. Comparative Analysis

A paired t -test was used to determine the statistical significance of the results for height estimation of the three different approaches. We chose a parametric test for all species because of the central limit theorem (CLT) for pine and birch ($N > 30$) and the normality in the residuals in all pairs for spruce ($N = 29$). The test observation among three approaches for height observation revealed both significant and insignificant results. For Pine [Measured-LiDAR: $t(32) = 3.09$, $p \leq 0.05$; Measured-DAP: $t(32) = 2.32$, $p < 0.05$; LiDAR-DAP: $t(32) = 0.40$, $p = 0.69$], for Spruce [Measured-LiDAR: $t(29) = 1.38$, $p = 0.18$; Measured-DAP: $t(29) = 2.00$, $p = 0.06$; LiDAR-DAP: $t(29) = 1.85$, $p = 0.07$] and for Birch [Measured-LiDAR: $t(67) = 5.38$, $p < 0.05$; Measured-DAP: $t(67) = 5.68$, $p \leq 0.05$; LiDAR-DAP: $t(67) = 2.20$, $p < 0.05$]. The paired t -test showed that with the exception of spruce, the height difference between the measured height and LiDAR/DAP height is statistically significant for the species studied. The t -test result found non-significance between LiDAR and DAP in pine and spruce. Overall, the height estimation from remote sensing methods is not statistically different from field measurements in spruce. In addition, both LiDAR

and DAP estimated similar heights in pine and spruce. In pine and birch, remote sensing methods underestimated the height of individual trees relative to field measurements.

We used a one-way ANOVA test to find out if the average height estimated from the three methods is significantly different for the studied species. The results for pine: [F (2,93) = 0.52, $p = 0.60$], spruce: [F (2,84) = 0.19, $p = 0.83$], birch: [F (2,198) = 2.91, $p = 0.06$] and all combined (+Aspen): [F (2,387) = 2.92, $p = 0.06$] suggested that there was no significant difference in mean height estimated for all three methods. However, the p values around the edge (0.05) suggest some differences which we assume are because of the temporal variation of one year between the remote sensing and field measurement.

Figure 7 shows the residuals of height differences from the three methods. The residuals related to DAP revealed few higher values in Pine and Birch. Moreover, there is a weak positive relationship of measured-LiDAR against measured tree height and measured-DAP against measured height in Birch and Pine. There is no correlation in Spruce. In addition, no relationship in residuals was found between LiDAR–DAP and LiDAR height in all species (Figure 7, last row).

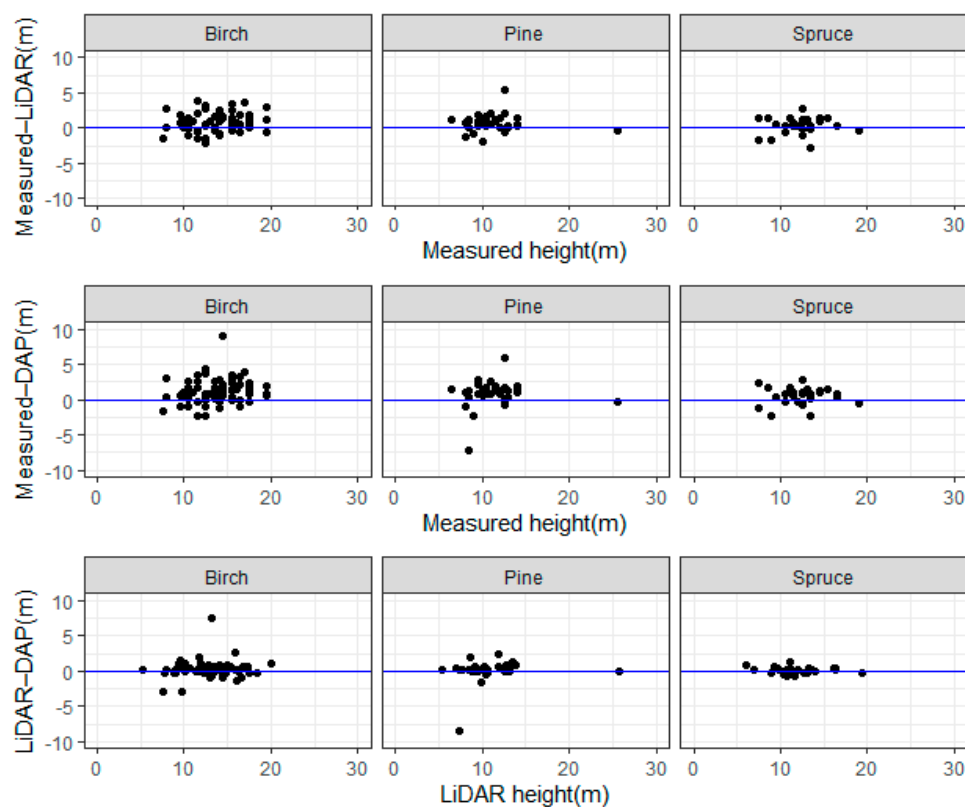


Figure 7. Height difference (m) between measured and LiDAR (first row), measured and DAP (second row), and LiDAR and DAP (last row).

4. Discussion

In this study, we examined the ability of modern remote sensing approaches, i.e., UAV LiDAR and DAP, to provide accurate estimations of individual tree height in a young forest in Finland. Manual selection of the individual trees in the LiDAR and DAP approaches and their identification in the field for reference measurements was possible due to the low density of the forest, the availability of DAP and LiDAR images, and the use of 3D point clouds. Moreover, manual matching of trees was also possible due to the selection of trees along the harvester trails. The manual location of individual trees has been carried out in previous studies [70,71]. In [70], up to 75 % of the trees were located correctly with an accuracy of 60 cm in a similar but denser pine–spruce–birch forest in Finland. In [71], individual trees detected using LiDAR were manually matched with field-measured trees

by digitally delineated tree crowns using GIS and the 3D LiDAR data viewer. High-density (>10 pulses/m²) LiDAR 3D point clouds were used as a reference to locate individual trees [71], which is also the case in our study.

We found that height estimated from DAP and LiDAR had a good correlation with field measured height. As shown in Table 4, a correlation coefficient (r) of 0.92 and 0.84 and RMSE of 1.44 and 1.92 were found, on average, between field measurements and LiDAR, and field measurements and DAP, respectively, for all species together. These correlation results are better than those of a previous study in *Eucalyptus* spp. plantations comparing LiDAR/DAP height with field measured height [53], where the correlation coefficient and RMSE between the field measurement and LiDAR were 0.69 and 2.84, respectively, and between the field measurement and DAP 0.66 and 2.80. Guerra-Hernández et al. [53] argued that the type of forest, more spherical shape of the crown than conifers, and topographically complex terrain causes inaccuracy in the formation of DEMs and estimation of tree height. Whereas, in our case, the better correlation in individual tree height between remote sensing and field measurement was mainly due to different tree densities and morphology and flat terrain of the area. The correlation coefficient between field measurements and LiDAR-detected individual tree height was close to 1 in [34], which was a study carried out in a pine-, spruce- and birch-dominated forest in Finland. However, the study was carried out in a sparsely populated mature forest. The paper noted that “the taller the tree, the more reliable was the ALS-based tree height” [34]. In our study, the correlation is a bit poorer, possibly due to a dominance of shorter and young trees. In addition, the tree heights in [34] were measured manually from ALS and TLS point clouds with the help of available tree maps, which differs from the data processing approach in this work. The differences in the comparison statistics could also be related to the nature of the forest stands, the tree density, and the crown cover.

In our study, the strongest correlation coefficients were between LiDAR and DAP tree height for spruce and birch. For pine, however, the correlation was strongest between the field measurement and LiDAR. It should be noted that the LiDAR estimated tree height showed a better correlation with field measurements than the DAP-based estimations, which is consistent with previous studies [23,32,33,38,45,52]. The overall performance and correlation accuracy (R^2 , RMSE, and bias) of the results in our study are better than the results from [45,52] and poorer than those presented in [23,32,33,38]. For example, in [38], a very significant statistical correlation with r values of 0.90–0.95 was found between LiDAR and DAP measurement when comparing height in different percentile height metrics. These values indicate a better correlation between the remote sensing methods and are in line with our study results. Conversely, the study by Sankey et al. [51] found DAP measurement (fixed-wing UAV multispectral image-based SfM point cloud data) had a better correlation ($r = 0.96$) with the field measurements than LiDAR ($r = 0.94$) in a sparsely populated ecotone.

The results from the paired t -test (Section 3.3.2) for field-LiDAR and field-DAP measurement for mean height estimation of pine and birch showed discrepancies between the field measurements and the remote sensing methods. Many factors may have affected the measurement performance of the studied methods. First, there was a temporal variation between the field measurement and remote sensing campaign. The difference of one year’s growing season between the observed and estimated height could have affected the result. The statistically insignificant paired t -test result for LiDAR and DAP for pine and spruce supports this supposition. However, the statistically insignificant result for every pair in spruce could be related to slow growth in the tree height in the year between the measurements. Second, it is unclear how accurately the trees were measured with the available field instruments. In a previous study of pine and spruce, ALS height estimation was found to be highly correlated with direct measurement (DIR) when compared to indirect measurements (IND), where the DIR was a measurement carried out on felled trees and IND (as in this study) was a measurement using field instruments on naturally existing trees [10]. However, all the estimation methods (three ALSs, DIR, and IND, five in total)

were not statistically different (Kruskal-Wallis test, $p = 0.92$). The authors of [10] raised the issue of selection of the true measurement and mentioned direct measurements on felled trees (DIR) as being an important factor affecting the accuracy of field and remote sensing surveys. This gives a valid reason to think about the importance of LiDAR implications in tree height measurements in comparison to traditional field measurements.

A case somewhat similar to our work is a study that compared DAP and ALS on similar species (Scots Pine, Norway Spruce, and Silver Birch) [32]. The paired t -test results in [32] presented strong evidence that the differences between the combinations of field, LiDAR, and DAP height measurement are statistically significant and that LiDAR/DAP height measurement tends to underestimate height compared to field data. It should be noted that the field and remote sensing data in [32] were collected during the same period. The authors further emphasized the role of the biophysical characteristics of each tree species and the complex and dense forest stands studied, which prevented the treetops from being clearly visible during field measurements. Moreover, the LiDAR and DAP data in [32] were processed differently because of slightly different outputs obtained for DAP-CHM. Hence, in some cases, it might be hardly fair to blame temporal difference alone for the significant t -test in comparison between the methods.

5. Conclusions

Utilization of LiDAR and DAP for height estimation is possible in sparsely populated stands of young trees. Moreover, there is no need for high-precision GNSS to locate an individual tree if high-resolution tree maps and 3D information of the plot are available for the given area. In this study, both the LiDAR- and DAP-derived tree heights were strongly correlated with the field height measurements in all species. However, LiDAR showed a greater correlation with field measurements than the DAP approach. The correlation between LiDAR and DAP is very strong for all species. All methods produced similar values for the height of spruce at the individual tree level. For pine and birch, however, there was a significant difference between field measurements and remote sensing methods. Both LiDAR and DAP displayed a tendency to underestimate tree heights compared to the field measurements. The presence of a few outliers estimated from DAP, specifically for pine and birch, resulted in abnormality in the residuals. However, overall average tree heights were not statistically different for the methods studied, which was seen in the ANOVA results for each species individually and combined.

Cost-effective 3D DAP methods may be the future of forest inventory at the individual tree level but, due to some inherent limitations, DAP cannot completely replace LiDAR technology. Nevertheless, DAP can be a reliable and economically viable method for collecting and updating information from young forests. Combining LiDAR and DAP measurement could be more effective for accurate estimation of height, diameter, and above-ground biomass of energy wood trees. The work in this paper considered spruce, birch, and pine in one Finnish forest stand; further study could examine larger areas with different ecological profiles to provide more information on the effectiveness of the methods and combinations of methods. Additionally, we suggest further study at an individual tree and stand level, specifically in young forests so that accurate information on biomass can be retrieved and the forest industry can contribute fully to the forthcoming energy transition.

Author Contributions: Conceptualization, A.G., J.P. and M.A.; methodology, A.G. and J.P.; software, A.G. and M.V.; formal analysis, A.G. and M.A.; writing—original draft preparation, A.G.; writing—review and editing, A.G., J.P., M.A., M.V. and T.R.; supervision, M.A. and T.R.; project administration, T.R.; funding acquisition, T.R. All authors have read and agreed to the published version of the manuscript.

Funding: This study is done as a part of the PUUSTI- "Puun tarjonnan kestävä edistäminen digitalisoinnin ja verkostoitumisen keinoin" project. The project is made possible through support from the Rural Development Programme for Mainland Finland (Project code: 101242). The project also received funding from the Suur-Savon Energiasäätiö.

Institutional Review Board Statement: Not applicable.

Informed Consent Statement: Not applicable.

Data Availability Statement: The study did not report any data. If required, the raw data can be made available on request.

Conflicts of Interest: The authors declare no conflict of interest. The funders had no role in the design of the study; in the collection, analyses, or interpretation of data; in the writing of the manuscript, or in the decision to publish the results.

Appendix A



Figure A1. UAV DAP with Sony camera mounted in GEODRONE X4L, and example of three consecutive images taken during campaign.

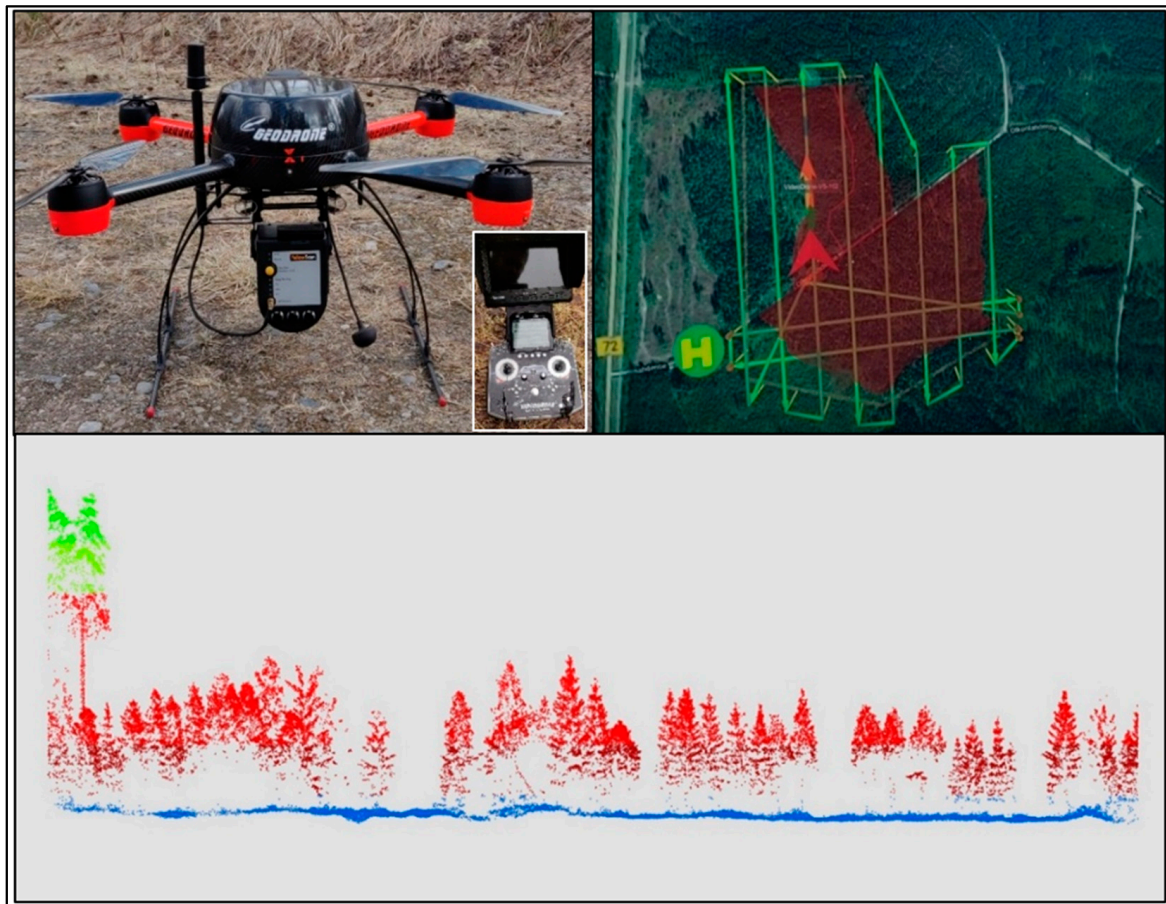


Figure A2. Yellow scan sensor mounted in GEODRONE X4L (UAV handler in the right corner), LiDAR flight path (green line) of the study area and profile view of 3D point cloud scanned from LiDAR.

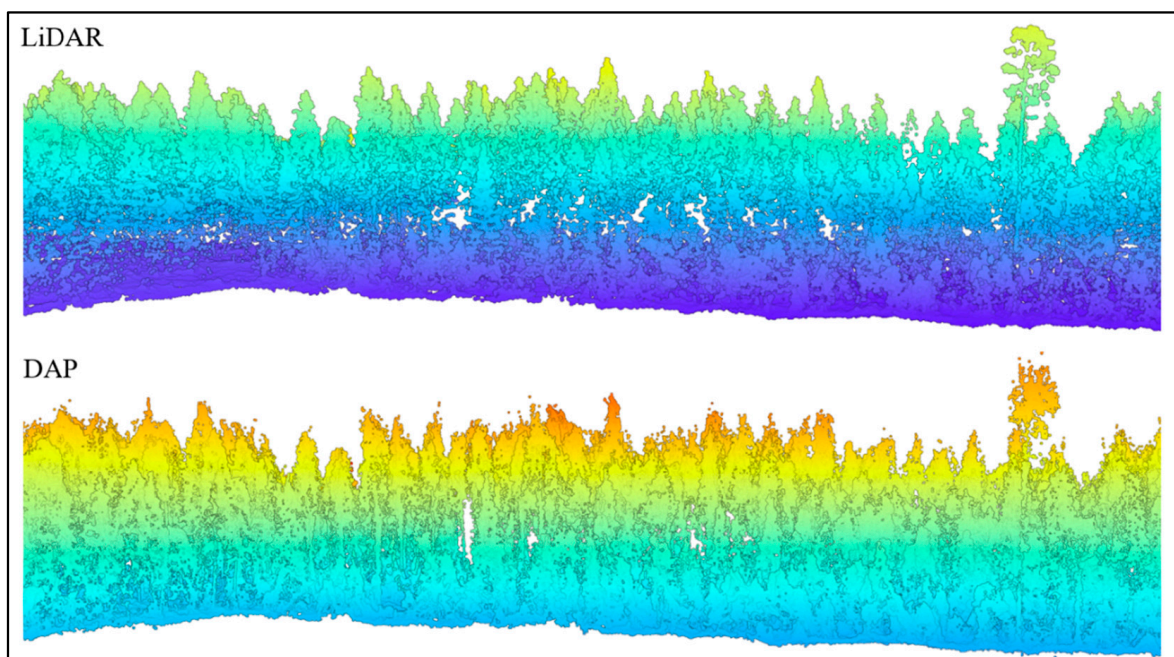


Figure A3. The cross section of 3D point clouds of a part of study area from LiDAR and DAP.



Figure A4. Field data collection: Orthophotographs, tree list map, caliper, tape, clinometer and measurement of tree height.

References

1. Official Statistics of Finland (OSF): Energy Supply and Consumption. Available online: https://www.stat.fi/til/ehk/2021/02/ehk_2021_02_2021-09-30_tie_001_en.html (accessed on 26 October 2021).
2. Anttila, P.; Nivala, V.; Salminen, O.; Hurskainen, M.; Kärki, J.; Lindroos, T.J.; Asikainen, A. Regional balance of forest chip supply and demand in Finland in 2030. *Silva Fenn.* **2018**, *52*, 9902. [CrossRef]
3. Ministry of Agriculture and Forestry. *Metsätalouden Kannustejärjestelmä 2020-Luvulla Työryhmän Muistio*; Ministry of Agriculture and Forestry: Helsinki, Finland, 2021; ISBN 9789523663978.
4. Petty, A.; Kärhä, K. Effects of subsidies on the profitability of energy wood production of wood chips from early thinnings in Finland. *For. Policy Econ.* **2011**, *13*, 575–581. [CrossRef]
5. Huttunen, R. *Government Report on the National Energy and Climate Strategy for 2030*; Ministry of Economic Affairs and Employment: Helsinki, Finland, 2017; ISBN 9789523271999. Available online: http://julkaisut.valtioneuvosto.fi/bitstream/handle/10024/79247/TEMjul_12_2017_verkkojulkaisu.pdf?sequence=1&isAllowed=y (accessed on 25 October 2021).
6. Finnish Forest Centre: Collection of Forest Resource Information. Available online: <https://www.metsakeskus.fi/en/open-forest-and-nature-information/collection-of-forest-resource-information> (accessed on 9 November 2021).
7. Kangas, A.; Astrup, R.; Breidenbach, J.; Fridman, J.; Gobakken, T.; Korhonen, K.T.; Maltamo, M.; Nilsson, M.; Nord-Larsen, T.; Næsset, E.; et al. Remote sensing and forest inventories in Nordic countries—roadmap for the future. *Scand. J. For. Res.* **2018**, *33*, 397–412. [CrossRef]
8. Vaglio Laurin, G.; Ding, J.; Disney, M.; Bartholomeus, H.; Herold, M.; Papale, D.; Valentini, R. Tree height in tropical forest as measured by different ground, proximal, and remote sensing instruments, and impacts on above ground biomass estimates. *Int. J. Appl. Earth Obs. Geoinf.* **2019**, *82*, 101899. [CrossRef]
9. Luoma, V.; Saarinen, N.; Wulder, M.A.; White, J.C.; Vastaranta, M.; Holopainen, M.; Hyypä, J. Assessing precision in conventional field measurements of individual tree attributes. *Forests* **2017**, *8*, 38. [CrossRef]
10. Sibona, E.; Vitali, A.; Meloni, F.; Caffo, L.; Dotta, A.; Lingua, E.; Motta, R.; Garbarino, M. Direct measurement of tree height provides different results on the assessment of LiDAR accuracy. *Forests* **2017**, *8*, 7. [CrossRef]
11. Stereńczak, K.; Mielcarek, M.; Wertz, B.; Bronisz, K.; Zajączkowski, G.; Jagodziński, A.M.; Ochał, W.; Skorupski, M. Factors influencing the accuracy of ground-based tree-height measurements for major European tree species. *J. Environ. Manag.* **2019**, *231*, 1284–1292. [CrossRef]
12. Vatandaşlar, C.; Zeybek, M. Extraction of forest inventory parameters using handheld mobile laser scanning: A case study from Trabzon, Turkey. *Meas. J. Int. Meas. Confed.* **2021**, *177*, 109328. [CrossRef]

13. Hyyppä, J.; Yu, X.; Hyyppä, H.; Vastaranta, M.; Holopainen, M.; Kukko, A.; Kaartinen, H.; Jaakkola, A.; Vaaja, M.; Koskinen, J.; et al. Remote Sensing Advances in Forest Inventory Using Airborne Laser Scanning. *Remote Sens.* **2012**, *4*, 1190–1207. [[CrossRef](#)]
14. Bienert, A.; Georgi, L.; Kunz, M.; Maas, H.-G.; von Oheimb, G. Comparison and Combination of Mobile and Terrestrial Laser Scanning for Natural Forest Inventories. *Forest* **2018**, *9*, 395. [[CrossRef](#)]
15. Hyyppä, E.; Kukko, A.; Kaijaluoto, R.; White, J.C.; Wulder, M.A.; Pyörälä, J.; Liang, X.; Yu, X.; Wang, Y.; Kaartinen, H.; et al. Accurate derivation of stem curve and volume using backpack mobile laser scanning. *ISPRS J. Photogramm. Remote Sens.* **2020**, *161*, 246–262. [[CrossRef](#)]
16. Liang, X.; Hyyppä, J.; Kaartinen, H.; Lehtomäki, M.; Pyörälä, J.; Pfeifer, N.; Holopainen, M.; Brolly, G.; Francesco, P.; Hackenberg, J.; et al. International benchmarking of terrestrial laser scanning approaches for forest inventories. *ISPRS J. Photogramm. Remote Sens.* **2018**, *144*, 137–179. [[CrossRef](#)]
17. Korpela, I.; Dahlin, B.; Schäfer, H.; Bruun, E.; Haapaniemi, F.; Honkasalo, J.; Ilvesniemi, S.; Kuutti, V.; Linkosalmi, M.; Mustonen, J.; et al. Single-tree forest inventory using lidar and aerial images for 3D treetop positioning, species recognition, height and crown width estimation. In Proceedings of the International Archives of the Photogrammetry, Remote Sensing and Spatial Information Sciences, Espoo, Finland, 12–14 September 2007; Volume XXXVI, part 3/W52. pp. 227–233.
18. Carr, J.C.; Slyder, J.B. Individual tree segmentation from a leaf-off photogrammetric point cloud. *Int. J. Remote Sens.* **2018**, *39*, 5195–5210. [[CrossRef](#)]
19. Mot, L.; Hong, S.; Charoenjit, K.; Zhang, H. Tree Height Estimation Using Field Measurement and Low-Cost Unmanned Aerial Vehicle (UAV) at Phnom Kulen National Park of Cambodia. In Proceedings of the 2021 9th International Conference on Agro-Geoinformatics (Agro-Geoinformatics 2021), Shenzhen, China, 26–29 July 2021; pp. 1–4.
20. Picos, J.; Bastos, G.; Míguez, D.; Alonso, L.; Armesto, J. Individual tree detection in a eucalyptus plantation using unmanned aerial vehicle (UAV)-LiDAR. *Remote Sens.* **2020**, *12*, 885. [[CrossRef](#)]
21. Xu, D.; Wang, H.; Xu, W.; Luan, Z.; Xu, X. LiDAR applications to estimate forest biomass at individual tree scale: Opportunities, challenges and future perspectives. *Forests* **2021**, *12*, 550. [[CrossRef](#)]
22. Peng, X.; Zhao, A.; Chen, Y.; Chen, Q.; Liu, H. Tree height measurements in degraded tropical forests based on UAV-LiDAR data of different point cloud densities: A case study on *Dacrydium pierrei* in China. *Forests* **2021**, *12*, 328. [[CrossRef](#)]
23. de Oliveira, L.F.R.; Lassiter, H.A.; Wilkinson, B.; Whitley, T.; Ifju, P.; Logan, S.R.; Peter, G.F.; Vogel, J.G.; Martin, T.A. Moving to automated tree inventory: Comparison of uas-derived lidar and photogrammetric data with manual ground estimates. *Remote Sens.* **2021**, *13*, 72. [[CrossRef](#)]
24. Dainelli, R.; Toscano, P.; Di Gennaro, S.F.; Matese, A. Recent advances in unmanned aerial vehicle forest remote sensing—A systematic review. Part i: A general framework. *Forests* **2021**, *12*, 327. [[CrossRef](#)]
25. Dainelli, R.; Toscano, P.; Di Gennaro, S.F.; Matese, A. Recent advances in unmanned aerial vehicles forest remote sensing—A systematic review. Part ii: Research applications. *Forests* **2021**, *12*, 397. [[CrossRef](#)]
26. Chisholm, R.A.; Rodríguez-Ronderos, M.E.; Lin, F. Estimating tree diameters from an autonomous below-canopy uav with mounted lidar. *Remote Sens.* **2021**, *13*, 2576. [[CrossRef](#)]
27. Næsset, E. Predicting forest stand characteristics with airborne scanning laser using a practical two-stage procedure and field data. *Remote Sens. Environ.* **2002**, *80*, 88–99. [[CrossRef](#)]
28. Goodwin, N.R.; Coops, N.C.; Culvenor, D.S. Assessment of forest structure with airborne LiDAR and the effects of platform altitude. *Remote Sens. Environ.* **2006**, *103*, 140–152. [[CrossRef](#)]
29. Wang, Y.; Koch, B. A Lidar Point Cloud Based Procedure for Vertical Canopy Structure Analysis and 3D Single Tree Modelling in Forest. *Sensors* **2008**, *8*, 3938–3951. [[CrossRef](#)] [[PubMed](#)]
30. Toth, C.; Józków, G. Remote sensing platforms and sensors: A survey. *ISPRS J. Photogramm. Remote Sens.* **2016**, *115*, 22–36. [[CrossRef](#)]
31. Wulder, M.A.; Bater, C.W.; Coops, N.C.; Hilker, T.; White, J.C. The role of LiDAR in sustainable forest management. *For. Chron.* **2008**, *84*, 807–826. [[CrossRef](#)]
32. Mielcarek, M.; Kamińska, A.; Stereńczak, K. Digital aerial photogrammetry (DAP) and airborne laser scanning (ALS) as sources of information about tree height: Comparisons of the accuracy of remote sensing methods for tree height estimation. *Remote Sens.* **2020**, *12*, 1808. [[CrossRef](#)]
33. Ganz, S.; Käber, Y.; Adler, P. Measuring Tree Height with Remote Sensing—A Comparison of Photogrammetric and LiDAR Data with Different Field Measurements. *Forest* **2019**, *10*, 694. [[CrossRef](#)]
34. Wang, Y.; Lehtomäki, M.; Liang, X.; Pyörälä, J.; Kukko, A.; Jaakkola, A.; Liu, J.; Feng, Z.; Chen, R.; Hyyppä, J. Is field-measured tree height as reliable as believed—A comparison study of tree height estimates from field measurement, airborne laser scanning and terrestrial laser scanning in a boreal forest. *ISPRS J. Photogramm. Remote Sens.* **2019**, *147*, 132–145. [[CrossRef](#)]
35. Goodbody, T.R.H.; Coops, N.C.; White, J.C. Digital Aerial Photogrammetry for Updating Area-Based Forest Inventories: A Review of Opportunities, Challenges, and Future Directions. *Curr. For. Rep.* **2019**, *5*, 55–75. [[CrossRef](#)]
36. Tuominen, S.; Pitkänen, T.; Balázs, A.; Kangas, A. Improving finnish multi-source national forest inventory by 3D aerial imaging. *Silva Fenn.* **2017**, *51*, 7743. [[CrossRef](#)]
37. Bohlin, J.; Wallerman, J.; Fransson, J.E.S. Forest variable estimation using photogrammetric matching of digital aerial images in combination with a high-resolution DEM. *Scand. J. For. Res.* **2012**, *27*, 692–699. [[CrossRef](#)]

38. Cao, L.; Liu, H.; Fu, X.; Zhang, Z.; Shen, X.; Ruan, H. Comparison of UAV LiDAR and Digital Aerial Photogrammetry Point Clouds for Estimating Forest Structural Attributes in Subtropical Planted Forests. *Forest* **2019**, *10*, 145. [CrossRef]
39. Mlambo, R.; Woodhouse, I.H.; Gerard, F.; Anderson, K. Structure from Motion (SfM) Photogrammetry with Drone Data: A Low Cost Method for Monitoring Greenhouse Gas Emissions from Forests in Developing Countries. *Forest* **2017**, *8*, 68. [CrossRef]
40. Tao, W.; Lei, Y.; Mooney, P. Dense point cloud extraction from UAV captured images in forest area. In Proceedings of the ICSDM 2011—2011 IEEE International Conference on Spatial Data Mining and Geographical Knowledge Services, Fuzhou, China, 29 June—1 July 2011; pp. 389–392.
41. Hao, Z.; Lin, L.; Post, C.J.; Mikhailova, E.A.; Li, M.; Chen, Y.; Yu, K.; Liu, J. Automated tree-crown and height detection in a young forest plantation using mask region-based convolutional neural network (Mask R-CNN). *ISPRS J. Photogramm. Remote Sens.* **2021**, *178*, 112–123. [CrossRef]
42. Hao, Z.; Lin, L.; Post, C.J.; Jiang, Y.; Li, M.; Wei, N.; Yu, K.; Liu, J. Assessing tree height and density of a young forest using a consumer unmanned aerial vehicle (UAV). *New For.* **2020**, *52*, 843–862. [CrossRef]
43. Panagiotidis, D.; Abdollahnejad, A.; Surový, P.; Chiteculo, V. Determining tree height and crown diameter from high-resolution UAV imagery. *Int. J. Remote Sens.* **2017**, *38*, 2392–2410. [CrossRef]
44. Kameyama, S.; Sugiura, K. Effects of differences in structure from motion software on image processing of unmanned aerial vehicle photography and estimation of crown area and tree height in forests. *Remote Sens.* **2021**, *13*, 626. [CrossRef]
45. Wallace, L.; Lucieer, A.; Malenovsky, Z.; Turner, D.; Vopěnka, P. Assessment of forest structure using two UAV techniques: A comparison of airborne laser scanning and structure from motion (SfM) point clouds. *Forests* **2016**, *7*, 62. [CrossRef]
46. Alonzo, M.; Andersen, H.E.; Morton, D.C.; Cook, B.D. Quantifying boreal forest structure and composition using UAV structure from motion. *Forests* **2018**, *9*, 119. [CrossRef]
47. Kotivuori, E.; Kukkonen, M.; Mehtätalo, L.; Maltamo, M.; Korhonen, L.; Packalen, P. Forest inventories for small areas using drone imagery without in-situ field measurements. *Remote Sens. Environ.* **2020**, *237*, 111404. [CrossRef]
48. Ullah, S.; Dees, M.; Datta, P.; Adler, P.; Schardt, M.; Koch, B. Potential of modern photogrammetry versus airborne laser scanning for estimating forest variables in a mountain environment. *Remote Sens.* **2019**, *11*, 661. [CrossRef]
49. Straub, C.; Stepper, C.; Seitz, R.; Waser, L.T. Potential of UltraCamX stereo images for estimating timber volume and basal area at the plot level in mixed European forests. *Can. J. For. Res.* **2013**, *43*, 731–741. [CrossRef]
50. Thiel, C.; Schmullius, C. Comparison of UAV photograph-based and airborne lidar-based point clouds over forest from a forestry application perspective. *Int. J. Remote Sens.* **2017**, *38*, 2411–2426. [CrossRef]
51. Sankey, T.; Donager, J.; McVay, J.; Sankey, J.B. UAV lidar and hyperspectral fusion for forest monitoring in the southwestern USA. *Remote Sens. Environ.* **2017**, *195*, 30–43. [CrossRef]
52. Moe, K.T.; Owari, T.; Furuya, N.; Hiroshima, T. Comparing individual tree height information derived from field surveys, LiDAR and UAV-DAP for high-value timber species in Northern Japan. *Forests* **2020**, *11*, 223. [CrossRef]
53. Guerra-Hernández, J.; Cosenza, D.N.; Rodriguez, L.C.E.; Silva, M.; Tomé, M.; Díaz-Varela, R.A.; González-Ferreiro, E. Comparison of ALS-and UAV(SfM)-derived high-density point clouds for individual tree detection in Eucalyptus plantations. *Int. J. Remote Sens.* **2018**, *39*, 5211–5235. [CrossRef]
54. Rodr, F.; Esteban, G.; Mart, S. UAV-Based LiDAR Scanning for Individual Tree Detection and Height Measurement in Young Forest Permanent Trials. *Remote Sens.* **2022**, *14*, 170. [CrossRef]
55. Llorens, J.; Gil, E.; Llop, J.; Queraltó, M. Georeferenced LiDAR 3D vine plantation map generation. *Sensors* **2011**, *11*, 6237–6256. [CrossRef]
56. Estornell, J.; Velázquez-Martí, B.; López-Cortés, I.; Salazar, D.; Fernández-Sarría, A. Estimation of wood volume and height of olive tree plantations using airborne discrete-return LiDAR data. *GIScience Remote Sens.* **2014**, *51*, 17–29. [CrossRef]
57. Wallace, L.; Musk, R.; Lucieer, A. An assessment of the repeatability of automatic forest inventory metrics derived from UAV-borne laser scanning data. *IEEE Trans. Geosci. Remote Sens.* **2014**, *52*, 7160–7169. [CrossRef]
58. Karpina, M.; Jarzabek-Rychard, M.; Tymków, P.; Borkowski, A. Uav-based automatic tree growth measurement for biomass estimation. In Proceedings of the International Archives of the Photogrammetry, Remote Sensing and Spatial Information Sciences—ISPRS Archives, Prague, Czech Republic, 12–19 July 2016; Volume XXIII ISPR, pp. 685–688.
59. Hentz, Á.M.K.; Silva, C.A.; Dalla Corte, A.P.; Netto, S.P.; Strager, M.P.; Klauberg, C. Estimating forest uniformity in Eucalyptus spp. and Pinus taeda L. stands using field measurements and structure from motion point clouds generated from unmanned aerial vehicle (UAV) data collection. *For. Syst.* **2018**, *27*, 17. [CrossRef]
60. Birdal, A.C.; Avdan, U.; Türk, T. Estimating tree heights with images from an unmanned aerial vehicle. *Geomat., Nat. Hazards Risk* **2017**, *8*, 1144–1156. [CrossRef]
61. Wu, D.; Johansen, K.; Phinn, S.; Robson, A.; Tu, Y.-H. Inter-comparison of remote sensing platforms for height estimation of mango and avocado tree crowns. *Int. J. Appl. Earth Obs. Geoinf.* **2020**, *89*, 102091. [CrossRef]
62. Hartley, R.J.L.; Leonardo, E.M.; Massam, P.; Watt, M.S.; Estarija, H.J.; Wright, L.; Melia, N.; Pearse, G.D. An assessment of high-density UAV point clouds for the measurement of young forestry trials. *Remote Sens.* **2020**, *12*, 4039. [CrossRef]
63. Chao, Z.; Liu, N.; Zhang, P.; Ying, T.; Song, K. Estimation methods developing with remote sensing information for energy crop biomass: A comparative review. *Biomass Bioenergy* **2019**, *122*, 414–425. [CrossRef]
64. Paikkatietoaineistot, Open Forest Information, Finnish Forest Center. Available online: <https://www.metsakeskus.fi/fi/avoimet-metsa-ja-luontotieto/aineistot-paikkatieto-ohjelmille/paikkatietoaineistot> (accessed on 10 September 2021).

65. Nuutinen, Y.; Miina, J.; Saksa, T.; Bergström, D.; Routa, J. Comparing the characteristics of boom-corridor and selectively thinned stands of scots pine and birch. *Silva Fenn.* **2021**, *55*, 10462. [[CrossRef](#)]
66. King, D.A. Linking tree form, allocation and growth with an allometrically explicit model. *Ecol. Modell.* **2005**, *185*, 77–91. [[CrossRef](#)]
67. Pix4D Drone Mapping Software. Swiss Fed Inst Technol Lausanne, Route Cantonale, Switzerland. 2014. Available online: <http://pix4d.com> (accessed on 25 May 2021).
68. Khosravipour, A.; Skidmore, A.K.; Isenburg, M.; Wang, T.; Hussin, Y.A. Generating pit-free canopy height models from airborne lidar. *Photogramm. Eng. Remote Sens.* **2014**, *80*, 863–872. [[CrossRef](#)]
69. Arbonaut Ltd. ArboLiDAR: Tools for Processing LiDAR and Satellite-Based Forest Inventory. Available online: <https://www.arbonaut.com/en/products/arbolidar> (accessed on 23 June 2021).
70. Kaartinen, H.; Hyypä, J.; Yu, X.; Vastaranta, M.; Hyypä, H.; Kukko, A.; Holopainen, M.; Heipke, C.; Hirschmugl, M.; Morsdorf, F.; et al. An international comparison of individual tree detection and extraction using airborne laser scanning. *Remote Sens.* **2012**, *4*, 950–974. [[CrossRef](#)]
71. Goldbergs, G.; Levick, S.R.; Lawes, M.; Edwards, A. Hierarchical integration of individual tree and area-based approaches for savanna biomass uncertainty estimation from airborne LiDAR. *Remote Sens. Environ.* **2018**, *205*, 141–150. [[CrossRef](#)]